

Supplementary Materials and Methods

Animal models of alcohol feeding. The Lieber DeCarli diet consisted of administering Micro Stabilized Rod Liq AC IRR (LD101A) and Maltodextrin IRR (9598) from TestDiet and 200 Proof Ethanol from Gold Shield in a specific combination following the manufacturer's feeding directions for two weeks. In brief, the caloric intake from ethanol was 0% on day 1, 10% on day 2 and 3, 20% on day 4 and 5, 30% from day 6 until the end of 6 weeks, and 36% for the last 2 weeks. Mortality of alcohol-fed mice was less than 25% in each ethanol-fed group. Pair-fed control mice received a diet with an isocaloric substitution of dextrose (LD101; TestDiet). Antibiotics treatment was started at 4 weeks after liquid diet feeding, and mice were gavaged daily until harvesting. The composition of antibiotics mixture has been described (Polymyxin B (150 mg/kg BW/day) and Neomycin (200 mg/kg BW/day))¹. Control mice were gavaged daily with an equal volume of vehicle (water). For acute alcohol treatment, mice were gavaged with 33% ethanol (Vol/Vol) using a dose of 5g/kg, sacrificed at 8 hours after administration, and MLCK phosphorylation was assessed in isolated intestinal epithelial cells. Age-matched female mice were used for the study except when stated otherwise. All animals received humane care in compliance with institutional guidelines.

Human samples. The selection criteria for the patient population with alcohol abuse has been described², and biopsies were taken from patients with endoscopically normal duodenums. Written informed consent was obtained from all patients and healthy controls. The study protocol was approved by the Ethics Committee of the Université Catholique de Louvain, in Brussels, Belgium, and of the VA San Diego Healthcare System. Duodenal biopsies were preserved in RNAlater (Qiagen) until RNA extraction using Trizol (Invitrogen). cDNA was synthesized and quantitative PCR was performed with the Step One Plus device (Applied Biosystems) by using SYBR Green PCR Master Mix (Applied Biosystems)³. The $\Delta\Delta$ CT method was used for quantification normalized to ribosomal protein L19 RNA (Rpl19; internal standard). Primers for human TNF α (NM_000594) were designed with Primer Express design

software (Applied Biosystems): 5'-GGAGAAGGGTGACCGACTCA-3';
5'-TGCCCAGACTCGGCAAAG-3'.

Histological analysis. Formalin fixed tissues were stained with hematoxylin and eosin and analyzed by microscopy. For hepatic lipid accumulation analysis, frozen section was cut and stained with oil red O. TUNEL staining was performed using a commercial kit (Millipore) following manufacturer's instructions.

Biochemical analysis. Plasma alanine aminotransferase (ALT) level was measured by Infinity ALT kit (Thermo Scientific). Plasma ethanol concentration was determined using the Ethanol Assay Kit (BioVision). Liver triglyceride levels were assessed using the triglyceride Liquid Reagents Kit (Pointe Scientific). Hepatic alcohol dehydrogenase (ADH) activity was measured using a commercial kit (BioVision).

Epithelial cell and lamina propria cell isolation. Isolation of intestinal epithelial and lamina propria cells has been described⁴. Lamina propria cells were collected by centrifugation, stained with PerCP-labeled CD11c, Pacific Blue-labeled CD11b, APC-labeled CD45.2, APC-labeled CD103, FITC-labeled Lys6C, PECy7-labeled F4/80, PE-labeled TNF α (all eBiosciences) and further analyzed by FACS analysis.

RNA extraction and realtime PCR analysis. RNA was extracted from mouse tissues using Trizol (Invitrogen). RNA was digested with DNase using the DNA-free kit (Ambion) and reverse transcribed using the High Capacity cDNA Reverse Transcription kit (ABI). Realtime qPCR was performed with Sybr Green (BioRad) supermix using primer sequences obtained from NIH qPrimerDepot. To determine the total bacterial load present in the cecum, the qPCR value of 16S for each sample was multiplied by the total amount of DNA per gram of cecal contents⁵.

Protein expression analysis. Liver microsomes were extracted as described⁶. Whole cell lysates were extracted from sterile liver, intestine or intestinal epithelial

cells, and western blot analysis was performed as described using primary antibodies for CYP2E1 (Millipore Corporation), *E. Coli* (DAKO), VDAC1 (Abcam), long isoform of p-MLCK [pS1760] (Invitrogen), iNOS (Santa Cruz), occludin (Invitrogen), TNFRI (Abcam), β -Actin (Sigma-Aldrich), and α -Tubulin (Santa Cruz). All materials used for measuring *E. Coli* proteins in the liver were sterile and pyrogen free. Frozen intestinal sections were stained using the primary antibody anti-occludin and a FITC-conjugated secondary antibody (all Invitrogen). Nuclei are stained with Hoechst (blue). To detect TNF α producing monocytes and macrophages in human duodenal biopsies and animal samples, tissue was stained with primary antibodies against CD68 (DAKO), F4/80 (eBioscience), Lys6C (Abcam) and TNF α (Abcam) and positive reactions were visualized using fluorescent labeled secondary antibodies. 5-6 random high power fields per slide were chosen for analysis, and double positive cells were expressed as percentage of CD68, F4/80 or Lys6C positive cells in the lamina propria. Nuclei are stained with DAPI (blue). Fecal albumin was determined by ELISA (Bethyl Labs) as described⁶. Plasma TNF α was measured using enzyme-linked immunosorbent assay (eBioscience) with a lower detection limit of 15.6 pg/mL.

LPS measurement. Plasma LPS level was measured by a commercial ELISA kit (Cloud-Clone Corp) according to the manufacturer's instruction.

FITC-dextran permeability assay. Mice were fed control or alcohol liquid diet for 2 weeks, and permeability was measured in an isolated jejunal loop as described in detail before⁷. In brief, after anesthesia, a midline laparotomy incision was made. An approximate 4cm long segment of the jejunum was created with two vascular hemoclips without disrupting the mesenteric vascular arcades. The length of intestine between the two clips was injected with 50ml FITC-dextran (4kDa; 100mg/ml; Sigma). After 1 hr, mice were sacrificed and fluorescence was measured in the plasma.

Statistical analysis. Student's *t*-test was used for statistical analysis. All data are presented as mean \pm SEM.

Supplementary Figure Legends

Supplementary Figure 1. Chronic ethanol administration does not elevate TNF α production in inflammatory cells in the ileum and colon of mice. C57BL/6 mice were orally fed a control or alcohol diet for 8 weeks (n = 3-4). Relative amount of TNF α ⁺ inflammatory cells isolated from the ileum or colon and analyzed by FACS. N.S.: no significance.

Supplementary Figure 2. Chronic ethanol administration does not elevate numbers of inflammatory cells in the intestine. C57BL/6 mice were orally fed a control or alcohol diet for 8 weeks (n = 3-4). Inflammatory cells isolated from the intestine and analyzed by FACS. *p < 0.05.

Supplementary Figure 3. Intestinal permeability in the jejunum of mice fed alcohol. C57BL/6 mice were orally fed a control or alcohol diet for 2 weeks (n = 20-21 in each group). FITC-dextran (50ml, 100mg/ml) was injected into an isolated jejunal loop. FITC was measured in the plasma 1 hr after injection. *p < 0.05.

Supplementary Figure 4. Intestinal decontamination reduces alcoholic liver disease. C57BL/6 mice were orally fed a control diet (n = 9), alcohol diet (n = 9) and alcohol diet plus antibiotics (ABX; n = 9). (A) Plasma ALT level. (B) Hepatic triglyceride content. (C) Representative liver sections after hematoxylin-eosin and oil red O staining (magnification x100). *p < 0.05.

Supplementary Figure 5. Intestinal decontamination reduces liver/body weight ratio but does not affect ethanol absorption. C57BL/6 mice were orally fed a control diet (n = 9), alcohol diet (n = 9) and alcohol diet plus antibiotics (ABX; n = 9). (A) Liver/body weight ratio. (B) Plasma ethanol concentration. *p < 0.05.

Supplementary Figure 6. Intestinal apoptosis and morphology following chronic alcohol feeding. C57BL/6 mice were orally fed a control or alcohol diet for 8

weeks (n = 3-5). (A) H&E staining and (B) TUNEL staining of jejunal sections. Female rat mammary gland after 3-5 days weaning (provided by the manufacturer) was used as positive control for TUNEL staining.

Supplementary Figure 7. TNFRI expression in liver and intestine. TNFRI protein expression was measured in isolated epithelial cells of the jejunum (A) and in the liver (B) of wild type (WT), TNFRI^{flxneo/flxneo} and VillinCre TNFRI^{flxneo/flxneo} mice.

Supplementary Figure 8. TNFRI gene expression in enterocytes is not affected by ethanol feeding. C57BL/6 mice were orally fed a control diet (n = 5) and alcohol diet (n = 4-5). Intestinal epithelial cells were isolated from jejunum, ileum and colon, and qPCR for TNFRI performed.

Supplementary Figure 9. TNF α expression is independent from intestinal TNFRI. Wild type (WT), TNFRI^{flxneo/flxneo} and VillinCre TNFRI^{flxneo/flxneo} mice were orally fed alcohol diet (n = 5) for 8 weeks. (A) TNF α mRNA level in the jejunum. (B) Quantification of F4/80 TNF α double positive cells in the jejunum as assessed by immunofluorescent staining. (C) Quantification of Lys6C TNF α double positive cells in the jejunum as assessed by immunofluorescent staining. N.S.: no significance.

Supplementary Figure 10. Plasma TNF α is below the detection level in control and alcohol fed mice. C57BL/6 mice were orally fed a control diet (n = 8) and alcohol diet (n = 9). Plasma TNF α levels were below the detection limit of 15.6 pg/ml.

Supplementary Figure 11. Reactivation of TNFRI on intestinal epithelial cells increases liver/body weight ratio but does not affect ethanol metabolism in TNFRI mutant mice after chronic alcohol feeding. Wild type (WT), TNFRI^{flxneo/flxneo} and VillinCre TNFRI^{flxneo/flxneo} mice were orally fed a control (ctrl; n = 3-4) and alcohol diet (n = 7-9). (A) Liver/body weight ratio. (B) Hepatic alcohol dehydrogenase (ADH) activity. (C) Representative western blot for hepatic microsomal CYP2E1. *p < 0.05.

Supplementary Figure 12. TNFR2 is dispensable for intestinal MLCK activation after alcohol administration. Wild type and TNFR2 deficient mice were gavaged with ethanol or dextrose as control once. Western blot for phosphorylated MLCK was performed (p-MLCK) in epithelial cells isolated from the jejunum.

Supplementary Figure 13. Liver/body weight ratio and hepatic ethanol metabolism in MLCK^{+/+} and MLCK^{-/-} mice. MLCK^{+/+} and MLCK^{-/-} littermate mice were orally fed a control (ctrl; n = 4) and alcohol diet (n = 10-14). (A) Liver/body weight ratio. (B) Hepatic alcohol dehydrogenase (ADH) activity. (C) Representative western blot for hepatic microsomal CYP2E1. *p < 0.05.

Supplementary Figure 14. MLCK does not affect hepatic chemokine expression after alcohol feeding. MLCK^{+/+} and MLCK^{-/-} littermate mice were orally fed a control (ctrl; n = 4) and alcohol diet (n = 8-10). Hepatic Ccl2 mRNA (A) and Ccl3 mRNA (B) levels. *p < 0.05.

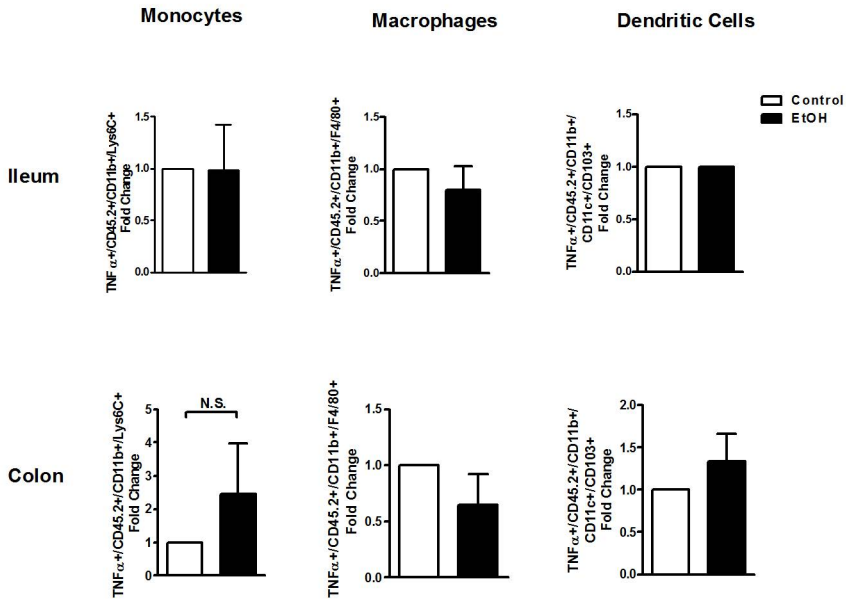
Supplementary Figure 15. Claudin-8 expression is differently regulated in TNFR1 mutant and MLCK knockout mice following alcohol feeding. (A) Wild type (WT), TNFR1^{flxneo/flxneo} and VillinCre TNFR1^{flxneo/flxneo} mice, (B) MLCK^{+/+} and MLCK^{-/-} mice were orally fed a control (n = 3-4) and alcohol diet (n = 7-10). Claudin-8 mRNA level was measured in the jejunum. *p < 0.05, N.S.: no significance.

Supplementary Figure 16. iNOS expression is regulated by TNFR1 but not MLCK after chronic alcohol feeding. Wild type (WT), TNFR1^{flxneo/flxneo} and VillinCre TNFR1^{flxneo/flxneo} mice; MLCK^{+/+} and MLCK^{-/-} mice were orally fed a control and alcohol diet for 8 weeks. iNOS protein levels were detected in the jejunum using western blotting.

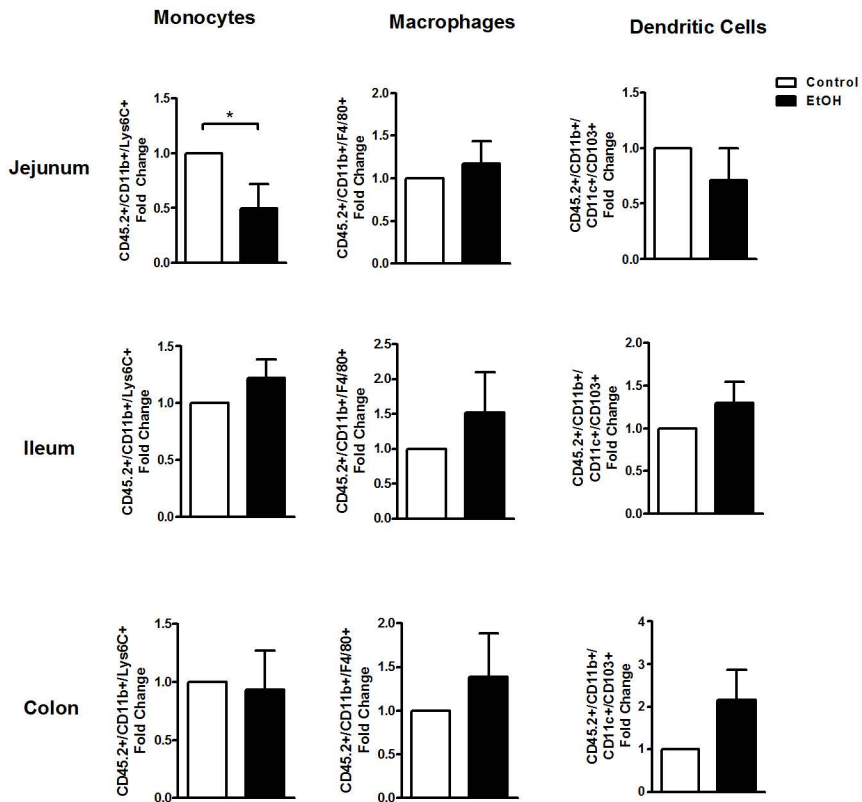
References

1. Adachi Y, Moore LE, Bradford BU, Gao W, Thurman RG. Antibiotics prevent liver injury in rats following long-term exposure to ethanol. *Gastroenterology* 1995;108:218-24.
2. Badaoui A, De Saeger C, Duchemin J, Gihousse D, de Timary P, Starkel P. Alcohol dependence is associated with reduced plasma and fundic ghrelin levels. *Eur J Clin Invest* 2008;38:397-403.
3. Starkel P, Bishop K, Horsmans Y, Strain AJ. Expression and DNA-binding activity of signal transducer and activator of transcription 3 in alcoholic cirrhosis compared to normal liver and primary biliary cirrhosis in humans. *Am J Pathol* 2003;162:587-96.
4. Hartmann P, Haimerl M, Mazagova M, Brenner DA, Schnabl B. Toll-like receptor 2-mediated intestinal injury and enteric tumor necrosis factor receptor I contribute to liver fibrosis in mice. *Gastroenterology* 2012;143:1330-40 e1.
5. Yan AW, Fouts DE, Brandl J, Starkel P, Torralba M, Schott E, et al. Enteric dysbiosis associated with a mouse model of alcoholic liver disease. *Hepatology* 2011;53:96-105.
6. Hartmann P, Chen P, Wang HJ, Wang L, McCole DF, Brandl K, et al. Deficiency of intestinal mucin-2 ameliorates experimental alcoholic liver disease in mice. *Hepatology* 2013;58:108-19.
7. Fouts DE, Torralba M, Nelson KE, Brenner DA, Schnabl B. Bacterial translocation and changes in the intestinal microbiome in mouse models of liver disease. *J Hepatol* 2012;56:1283-92.

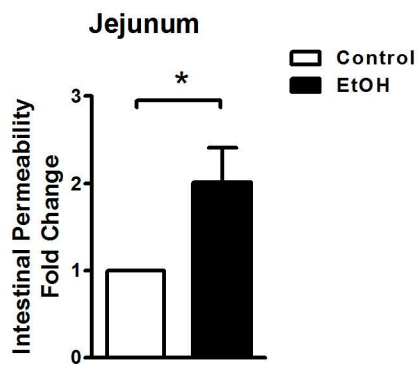
Supplementary Figure 1



Supplementary Figure 2

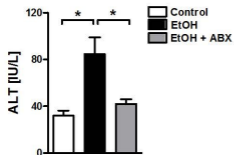


Supplementary Figure 3

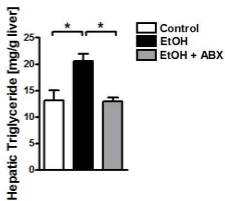


Supplementary Figure 4

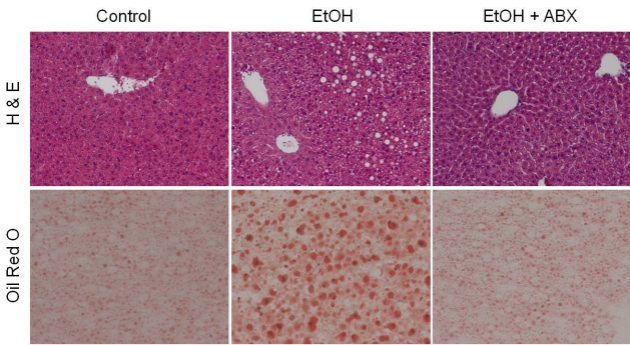
A



B

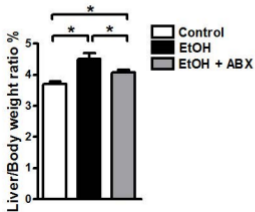


C

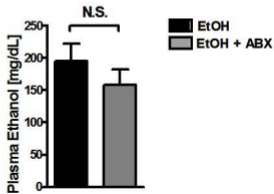


Supplementary Figure 5

A



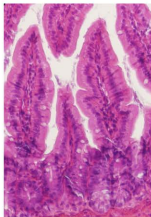
B



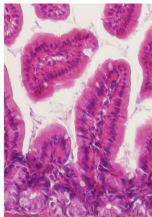
Supplementary Figure 6

A

Control

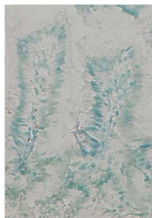


EtOH

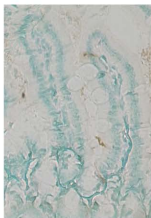


B

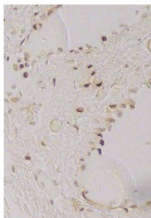
Control



EtOH

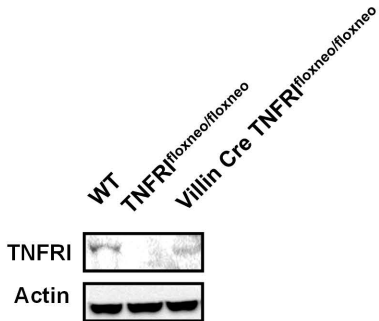


Positive Control

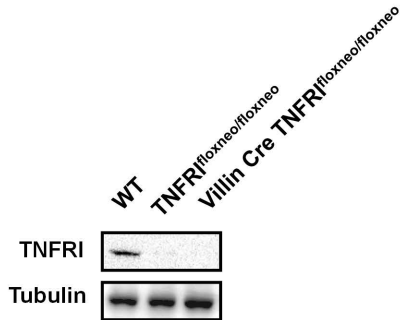


Supplementary Figure 7

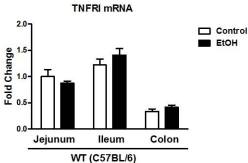
A



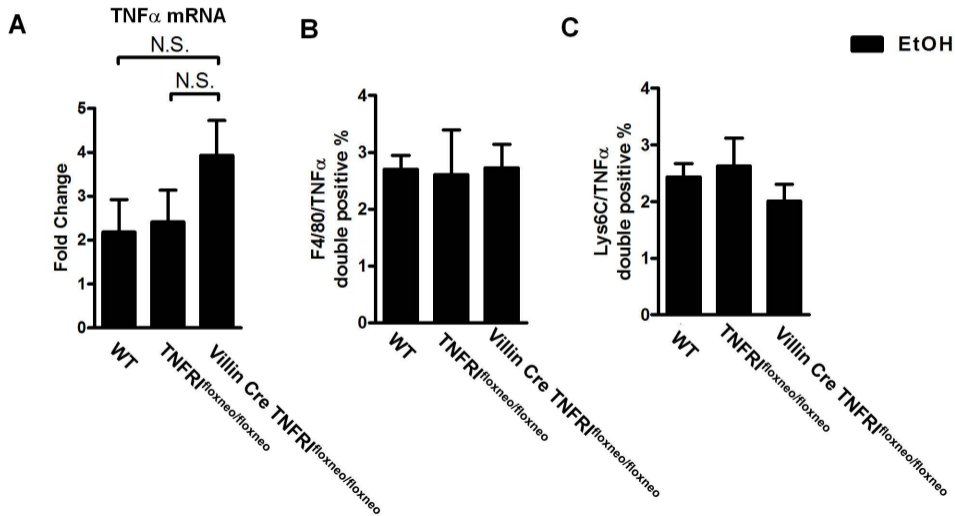
B



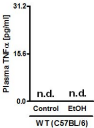
Supplementary Figure 8



Supplementary Figure 9

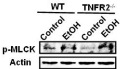


Supplementary Figure 10



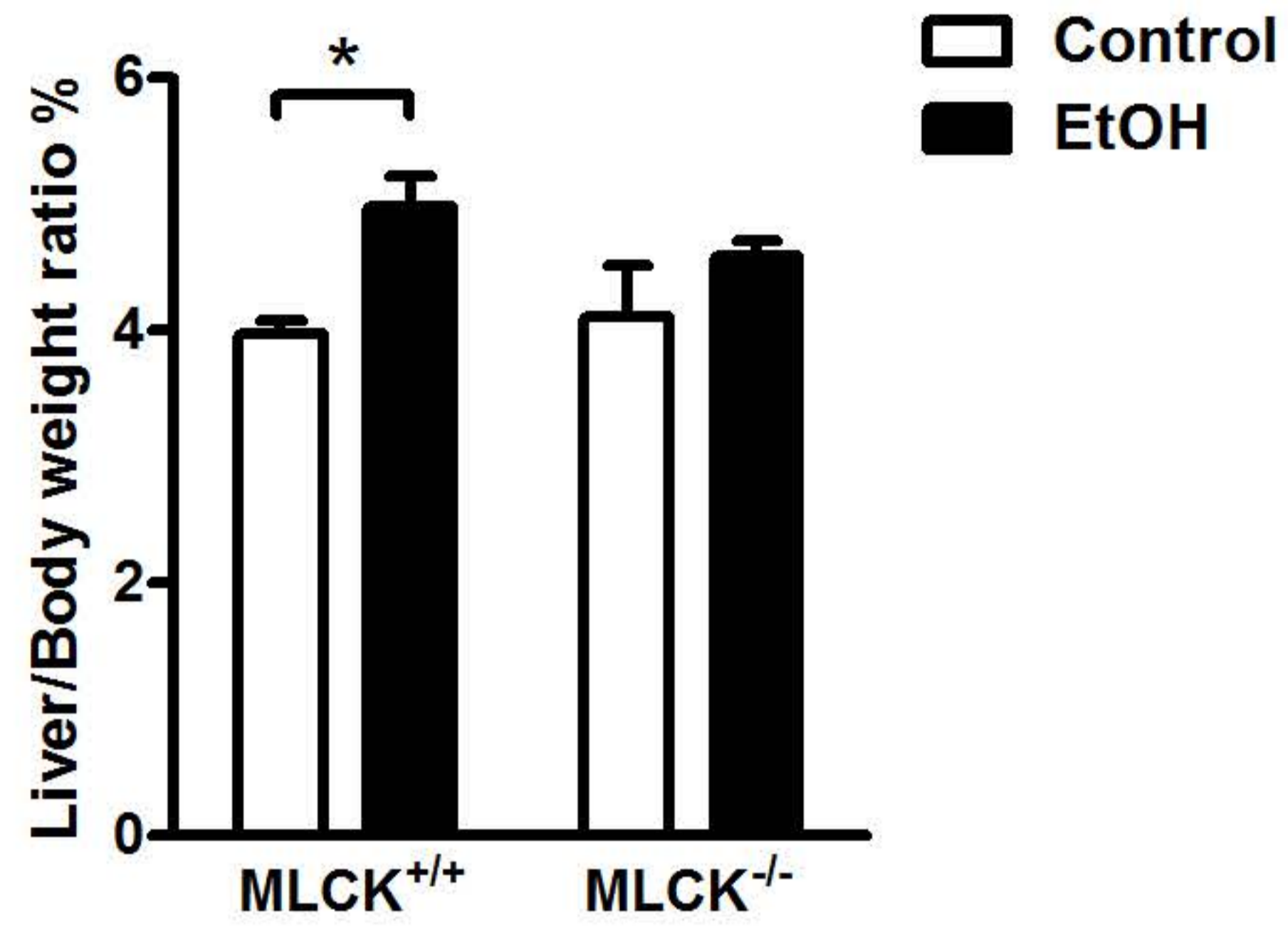
Supplementary Figure 12

A

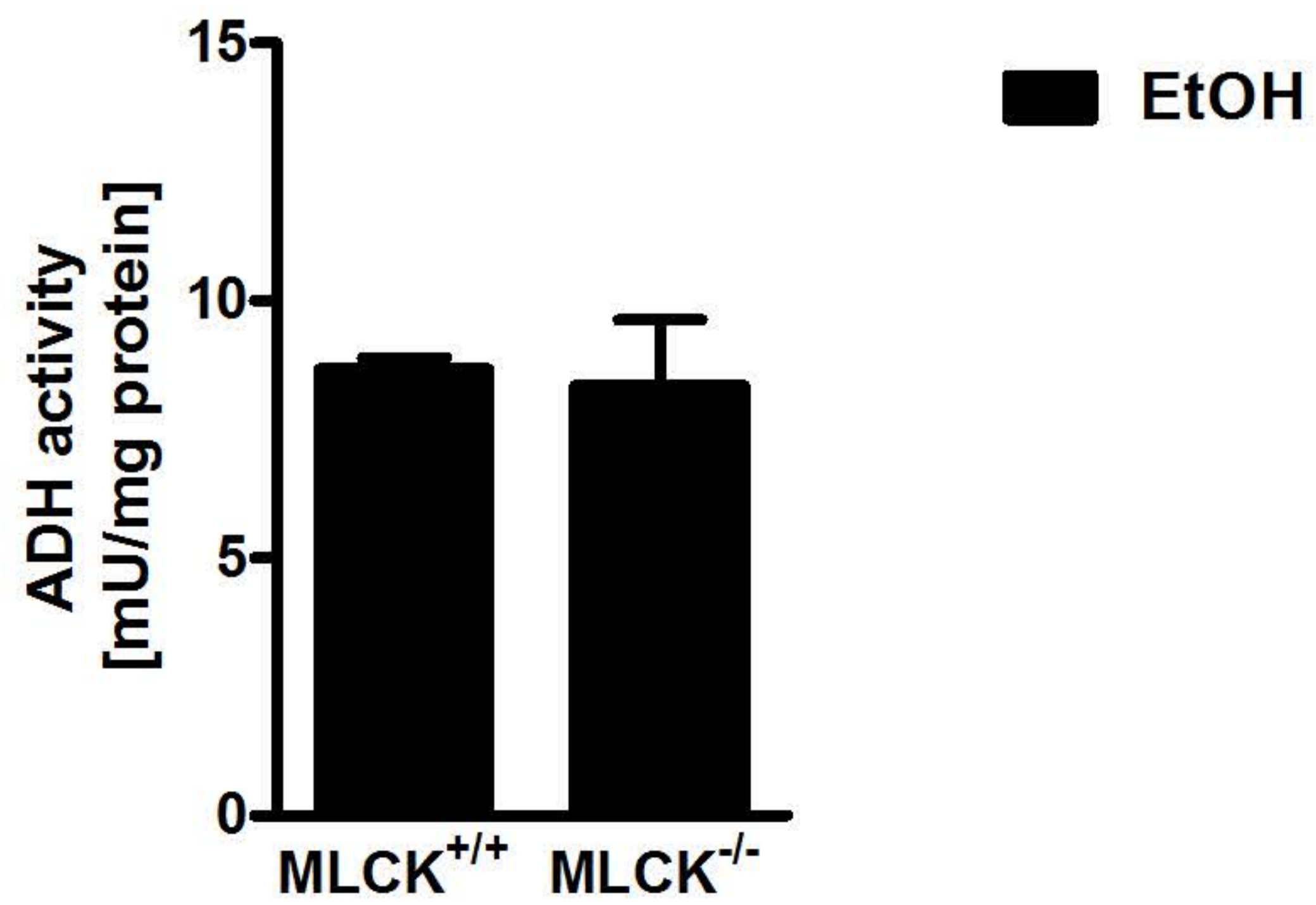


Supplementary Figure 13

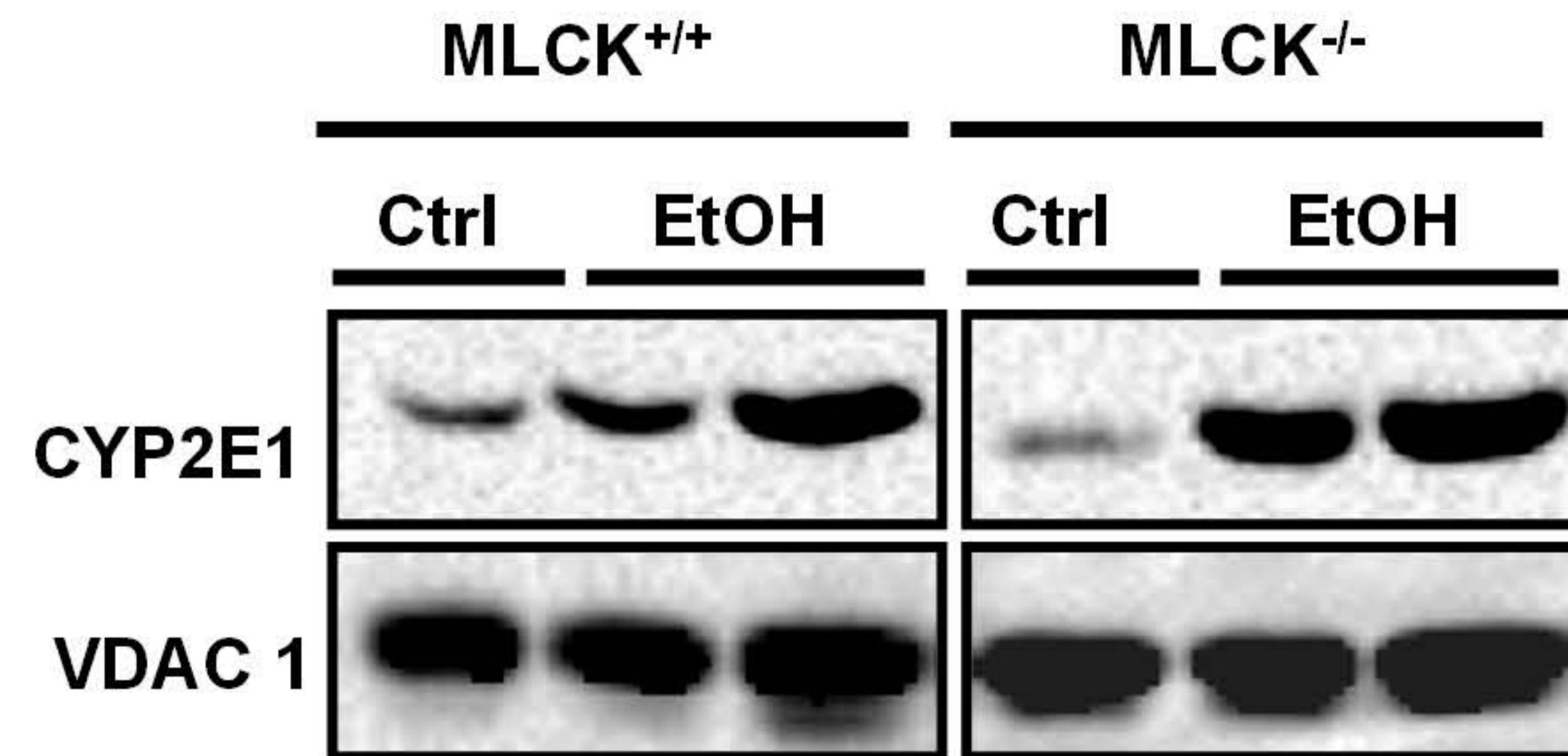
A



B

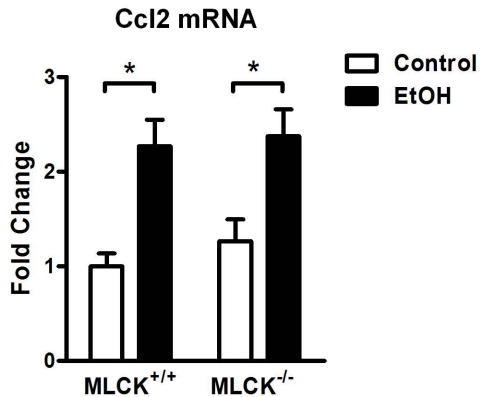


C

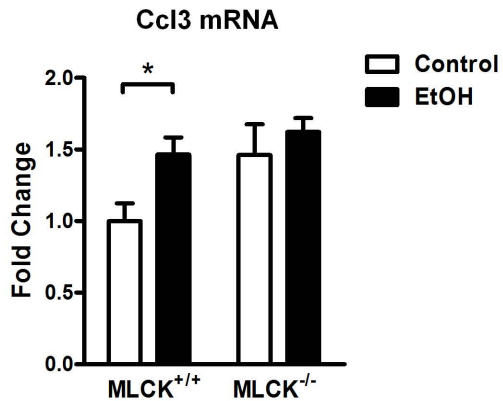


Supplementary Figure 14

A

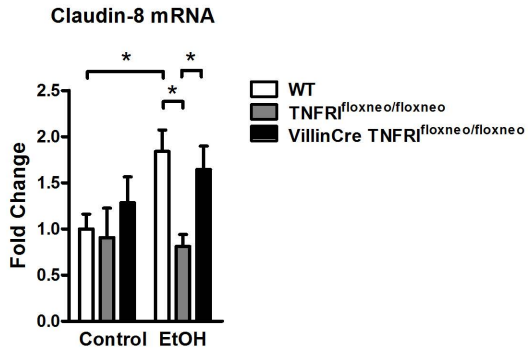


B

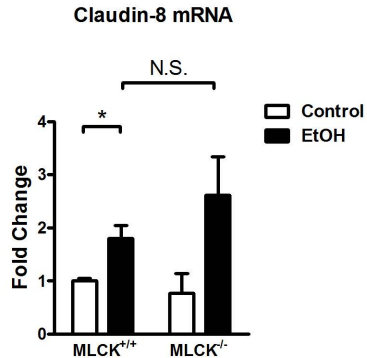


Supplementary Figure 15

A

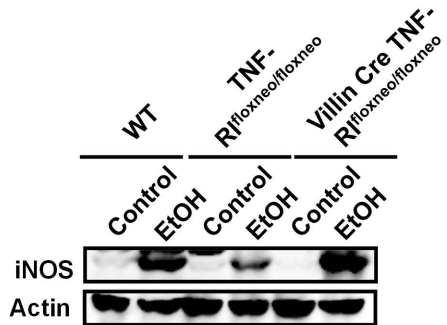


B



Supplementary Figure 16

A



B

